Redox Biology 36 (2020) 101641

Contents lists available at ScienceDirect

Redox Biology

journal homepage: www.elsevier.com/locate/redox

Research Paper

Myeloperoxidase-derived damage to human plasma fibronectin: Modulation by protein binding and thiocyanate ions (SCN^-)

Siriluck Vanichkitrungruang [a,b,c], Christine Y. Chuang [c], Clare L. Hawkins [a,b,c], Michael J. Davies [a,b,c,*]

[a] The Heart Research Institute, Newtown, NSW, Australia
[b] Faculty of Medicine, The University of Sydney, NSW, Australia
[c] Department of Biomedical Sciences, Panum Institute, University of Copenhagen, Denmark

ARTICLE INFO

Keywords:
Extracellular matrix
Hypochlorous acid
Myeloperoxidase
Hypothiocyanous acid
Fibronectin
Protein oxidation
Endothelial cell

ABSTRACT

Endothelial cell dysfunction is an early event in cardiovascular disease and atherosclerosis. The origin of this dysfunction is unresolved, but accumulating evidence implicates damaging oxidants, including hypochlorous acid (HOCl), a major oxidant produced by myeloperoxidase (MPO), during chronic inflammation. MPO is released extracellularly by activated leukocytes and binds to extracellular molecules including fibronectin, a major matrix glycoprotein involved in endothelial cell binding. We hypothesized that MPO binding might influence the modifications induced on fibronectin, when compared to reagent HOCl, with this including alterations to the extent of damage to protein side-chains, modified structural integrity, changes to functional domains, and impact on naïve human coronary artery endothelial cell (HCAEC) adhesion and metabolic activity. The effect of increasing concentrations of the alternative MPO substrate thiocyanate (SCN^-), which might decrease HOCl formation were also examined. Exposure of fibronectin to MPO/H_2O_2/Cl^- is shown to result in damage to the functionally important cell-binding and heparin-binding fragments, gross structural changes to the protein, and altered HCAEC adhesion and activity. Differences were observed between stoichiometric, and above-stoichiometric MPO concentrations consistent with an effect of MPO binding to fibronectin. In contrast, MPO/H_2O_2/SCN^- induced much less marked changes and limited protein damage. Addition of increasing SCN^- concentrations to the MPO/H_2O_2/Cl^- system provided protection, with 20 μM of this anion rescuing damage to functionally-important domains, decreasing chemical modification, and maintaining normal HCAEC behavior. Modulating MPO binding to fibronectin, or enhancing SCN^- levels at sites of inflammation may therefore limit MPO-mediated damage, and be of therapeutic value.

1. Introduction

The heme enzyme myeloperoxidase (MPO) generates the potent oxidizing species hypochlorous acid (HOCl, the major active component of household bleach) at sites of inflammation using hydrogen peroxide (H_2O_2) and chloride ions (Cl^-) (reviewed [1]). This enzyme is released into the phagolysosomes of activated neutrophils, monocytes and some tissue macrophage-like cells, to kill invading pathogens [2]; some MPO is also released extracellularly. This enzyme can also utilize other halide ions including bromide (Br^-) and iodide (I^-), and the pseudohalide thiocyanate (SCN^-) to give hypobromous acid (HOBr), hypoiodous acid (HOI) and hypothiocyanous acid (HOSCN), respectively (reviewed [1,3]). HOSCN can be formed to a significant extent under some conditions, due to the higher specificity constant of MPO for SCN^- compared to Cl^- [4], and the high rate constant for HOSCN formation when compared to HOCl (rate constants, k, for reaction with MPO Compound I of 9.6×10^6 and 2.5×10^4 M^{-1} s^{-1} for SCN^- and Cl^-, respectively [5]). At neutral pH values HOCl is present as a near equal mixture of the neutral (HOCl) and ionized forms ($^-$OCl), whereas HOSCN is predominantly present as the ionized anion $^-$OSCN (see Ref. [1,3]). From here on, HOCl and HOSCN are used to describe these physiological mixtures.

HOCl formation by MPO is important in leukocyte-mediated pathogen clearance [2]. However, the release of MPO extracellularly, due to aberrant processing, cell lysis, and neutrophil extracellular trap (NET) formation, can result in host tissue damage [6–9]. This has been linked with many inflammatory diseases, and elevated levels of MPO-mediated biomarkers (e.g. 3-chlorotyrosine, from chlorination of the amino acid

* Corresponding author. Department of Biomedical Sciences, Panum Institute, University of Copenhagen, Denmark.
E-mail address: davies@sund.ku.dk (M.J. Davies).

https://doi.org/10.1016/j.redox.2020.101641
Received 20 May 2020; Received in revised form 3 July 2020; Accepted 6 July 2020
Available online 9 July 2020

Abbreviations

ABTS	2,2′-azino-bis(3-ethylbenzothiazoline-6-sulphonic acid)
BSA	bovine serum albumin
CBF	cell-binding fragment
di-Trp	covalently cross-linked Trp residues
di-Tyr	the cross-linked species 3,3′-*o,o*-dityrosine
DTT	dithiothreitol
ECM	extracellular matrix
EDA	extra domain A
HCAEC	human coronary artery endothelial cells
HBF	heparin-binding fragment
HOCl	the physiological mixture of hypochlorous acid and its anion $^{-}$OCl
HOSCN	the physiological mixture of hypothiocyanous acid and its anion $^{-}$OSCN
HRP	horseradish peroxidase
mAb	monoclonal antibody
MMP	matrix metalloproteinase
MPO	myeloperoxidase
MTS	3-(4,5-dimethylthiazol-2-yl)-5-(3-carboxymethoxyphenyl)-2-(4-sulfophenyl)-2H-tetrazolium
pAb	polyclonal antibody
PBS	phosphate-buffered saline
PBST	PBS with added Tween 20
TBST	Tris-buffered saline with added Tween 20
THF	tetrahydrofuran
TIMP	tissue inhibitor of MMPs

tyrosine, and chlorinated DNA bases) are associated with the severity of the pathology (reviewed [1,3,10]).

HOCl can induce necrosis, apoptosis and other forms of cell death, and also modify extracellular targets, including plasma proteins and the extracellular matrix (ECM) (reviewed [1]). Such damage appears to be particularly prevalent as extracellular compartments typically have much lower levels of antioxidant defenses and repair mechanisms [11], and may be of particular significance as ECM proteins play a key role in defining tissue structure, bind materials such as lipoproteins and other proteins/enzymes [12], and control key aspects of cell function, including adhesion, proliferation and metabolic activity [13]. Many extracellular proteins are present at high concentration (e.g. 60–80 g protein L^{-1} for plasma) and have relatively long half-lives, such that they accumulate damage. Thus up to 70% of the damage detected in human artery atherosclerotic lesions has been reported to be present on ECM proteins [14], including laminins, fibronectin and perlecan [15–20]. Collagens (e.g. Type IV in basement membranes, and Types I and III in interstitial matrix [21]) appear to be less important targets [22], due to their low levels of HOCl-reactive side-chains. The damage induced by HOCl and MPO on fibronectin and laminins, has been examined by LC-MS protein mass mapping, with modifications detected at multiple sites [17,18]. The uneven distribution of the observed modifications, the observed differences between reagent HOCl and the enzyme system, and also between proteins, has been suggested to arise from MPO binding, possibly via ionic interactions, to specific sites and proteins including fibronectin [19,23–25].

Fibronectin is a key glycoprotein comprised of two near-identical monomers (220–270 kDa, dimer mass ~460 kDa) bound by two disulfide bonds at the carboxyl termini [26,27]. The protein exists in two major isoforms: a soluble plasma form primarily synthesized and released by hepatocytes, and a less soluble cellular isoform synthesized by multiple cells including endothelial cells and fibroblasts [28]. These forms differ primarily by the presence of extra domains (EDA and EDB) in the cellular form. Plasma fibronectin plays a key role in the coagulation cascade, via its interactions with fibrin, and in wound healing where it is a key component of the temporary ECM, and mediates cell adhesion [28]. Basement membranes are a specialized ECM which underlies and supports endothelial and epithelial cells in most tissues. Cellular fibronectin is a key component of some basement membranes, including those of the vasculature, and is also found in some interstitial matrices. Fibronectin plays a key role in ECM assembly and function, including cell adhesion (by interacting with cell surface receptors and integrins) and proliferation [26,28–30], and is particularly abundant in human atherosclerotic lesions [26,27].

Although there is clear evidence for a role of HOCl in the modification of biological materials, including the ECM *in vivo*, less is known about the significance of SCN^{-}, and HOSCN derived from it, in inflammatory pathologies. SCN^{-} may be of therapeutic value in reducing the extent of HOCl-induced damage, as HOSCN is a much less reactive and more selective oxidant [31], and can be detoxified by intracellular antioxidant systems [32]. SCN^{-} supplementation has been reported to be beneficial in animal models of cystic fibrosis, with evidence for decreased inflammation, pro-inflammatory cytokine levels, bacterial load and glutathione sulfonamide levels, a biomarker of HOCl production [33,34]. Elevated levels of SCN^{-} have also been shown to decrease MPO-mediated damage to human plasma proteins [35], modulate lesion formation in atherosclerosis-prone mice [36,37] and rabbits [38], and be associated with increased long-term survival in subjects who have suffered a first myocardial infarction [39].

In the light of these data, we hypothesized that: 1) damage induced by a $MPO/H_2O_2/Cl^{-}$ system on human plasma fibronectin would differ to that induced by $MPO/H_2O_2/SCN^{-}$, due to differences in the chemistry of HOCl versus HOSCN, and also as a result of MPO binding to fibronectin, and 2) that damage generated by $MPO/H_2O_2/Cl^{-}$ might be modulated by increasing SCN^{-} concentrations, due to a switch from HOCl to HOSCN generation. Decreased damage in the presence of SCN^{-}, could therefore rationalize the positive effects of high levels of SCN^{-} detected in the pathologies described above.

2. Materials and methods

2.1. Materials

Chemicals and reagents were from Sigma Aldrich/Merck (Castle Hill, NSW, Australia; Søborg, Denmark) unless stated otherwise. The water used to prepare solutions was filtered through a four-stage Millipore MilliQ system ("MilliQ water"), with Chelex resin used to remove trace metal ions. Phosphate-buffered saline (PBS, 20x stock), sodium carbonate, Tris, and 37% (w/v) formaldehyde were purchased from Amresco (Solon, OH, USA). Sodium chloride was from UNIVAR (Redmond, Washington, USA). Human polymorphonuclear leukocyte-derived MPO was purchased from Planta Natural Products (Vienna, Austria). NuPAGE 3–8% w/v Tris-acetate gels, NuPAGE Tris-acetate SDS Running buffer (20x stock; LA0041), HiMark™ pre-stained and unstained high molecular mass standards, iBlot 2, and polyvinylidene difluoride (PVDF) membrane transfer stacks were from Life Technologies (Slangerup, Denmark). Western Lightning Plus-Electrochemiluminescence reagent for detection of proteins on immunoblots was obtained from PerkinElmer (Waltham, MA, USA). The antibodies used were: a mouse monoclonal antibody (mAb) against the fibronectin cell-binding fragment (CBF) (clone A17; Abcam, Cambridge, UK), a mouse mAb against the heparin-binding fragment (HBF; clone A32; Rockford, USA), a mouse mAb against the extra domain A (EDA) splice variant (clone 3E2, Sigma, Denmark), a mouse mAb (clone

2D10G9) raised against HOCl-modified epitopes (kindly provided by Prof. Ernst Malle, Medical University of Graz, Austria) [40], and a polyclonal rabbit anti-fibronectin antibody (pAb) (ab2413; Abcam, Cambridge, UK). CellTiter 96 ® Aqueous One Solution Assay for cellular metabolic activity measurements was obtained from Promega (Wisconsin, USA).

2.2. ELISA

High-binding 96-well plates were coated with purified human plasma (50 μL, 0.02 μM) overnight at 4 °C, and then washed twice with PBS. Our previous studies indicate that under these conditions ~96% of the fibronectin adheres to the plates [16]. For oxidant treatment, the wells were incubated with 0.02 μM of MPO (i.e. equimolar with the fibronectin concentration), 100 mM Cl^-, variable concentrations of SCN^- (0–500 μM) and lastly 32 μM H_2O_2 (added as 4 aliquots of 8 μM) in a total volume of 50 μL, for 2 h at 37 °C. The samples were washed twice with PBS to remove any residual oxidant, and subsequently blocked with 0.1% (w/v) casein in PBS for 1 h at 21 °C on a rocking platform. The wells were then washed twice with PBS containing Tween 20 (PBST, 0.01% (v/v)) and probed using the antibodies against the CBF (A17, 1:10000), HBF (A32, 1:2000), EDA (3E2, 1:1000) and HOCl-generated epitopes (2D10G9, 1:100) by incubation with the primary antibodies diluted in 0.1% (w/v) casein in PBS overnight at 4 °C. The wells were washed twice with PBST, prior to incubation with a secondary rabbit anti-mouse antibody conjugated with alkaline phosphatase (1:1000, Abcam) and *p*-nitrophenylphosphate solution (Merck) at 21 °C for 20 min. The optical absorbance of the resulting *p*-nitrophenolate anion was determined using a Spectra Max i3x microplate reader (Molecular Devices). The alkaline phosphatase system was used, rather than HRP/ABTS/H_2O_2, as both HRP and MPO can react with H_2O_2 potentially resulting in erroneous absorbance values (cf [19]).

2.3. SDS-PAGE, silver staining and immunoblotting

Purified human plasma fibronectin (0.2 μM in 0.1 M phosphate buffer, pH 7.4) was left untreated (control), treated with 0.02 or 0.1 μM MPO/100 mM Cl^- and increasing concentrations of H_2O_2 (0, 20, 40, 80, 120, 160 μM, added in aliquots as described above) and incubated for 2 h at 37 °C. Alternatively, fibronectin (as above) was treated with 0.2 μM MPO, 20 or 500 μM SCN^- and increasing concentrations of H_2O_2 (0, 20, 40, 80, 120, 160 μM), and incubated for 2 h at 37 °C. Samples were prepared for analysis by addition of NuPAGE® LDS Sample Buffer (4x stock), in the absence or presence of NuPAGE® Sample Reducing Buffer (10x stock) following the manufacturer's instructions, and denatured for 10 min at 70 °C. Aliquots were then loaded onto 1 mm NOVEX® 3–8% Tris-Acetate Gels (0.25–1.25 μg protein per well) with Tris-Acetate SDS Running buffer, and run at 160 V at a constant current for 70 min. Gels were subsequently developed using silver staining [41], or immunoblotted to PVDF membranes to examine the presence of functional or damaged epitopes.

For the immunoblotting analyses, proteins were transferred to PVDF membranes using an iBlot 2® Gel Transfer device (Life Technologies), and blocked using 1% (w/v) BSA in TBST for 1 h followed by incubation with primary antibodies (overnight, 4 °C) at the dilutions given above. The membranes were then washed with TBST for 5 min before incubation with a secondary HRP-conjugated sheep anti-mouse IgG antibody (1:5000, 1 h, 21 °C). The membranes were then washed and chemiluminescence recorded using either a Bio-rad Chemidoc™ or a Syngene G:Box XR5 system.

2.4. Cell culture

Human coronary artery endothelial cells (HCAEC, from 3 independent donors; Cell Applications, San Diego, CA, USA) were cultured using MesoEndo Endothelial Cell Growth Media (Cell Applications) and used at passages 4–6. HCAEC were removed from the culture plates by treatment with 0.1% (w/v) trypsin-EDTA for 1 min at 37 °C before deactivation of trypsin with added growth media. The cells were then pelleted by centrifugation (5 min, ~232 *g*), the supernatant removed by aspiration, and the cells resuspended in media before seeding overnight at a density of 2×10^5 cells mL^{-1}.

2.5. Cell adhesion and metabolic activity assays

Tissue culture plates (clear bottom, 96-wells) were coated with purified human plasma fibronectin (0.02 μM) as described above. The bound protein was exposed to the different oxidation systems (as above) for 2 h at 37°C, and then washed twice with PBS. The wells were blocked to minimize non-specific binding using 3% (w/v) BSA in PBS (1 h, 37 °C), and subsequently washed twice with sterile PBS. HCAEC (2.0×10^5 cells mL^{-1}) were pre-loaded with 5 μM calcein-AM for 30 min at 37 °C, with residual probe removed by washing with pre-warmed medium (Cell Applications). Calcein-AM loaded cells (12500 per well) were added and incubated in a tissue culture incubator at 37 °C for 90 min. The plates were then rinsed twice with sterile PBS (containing Ca^{2+} and Mg^{2+}) to remove non-adherent cells, and fluorescence arising from cleavage (by intracellular esterases of viable cells) of the non-fluorescent parent to the fluorescent product, recorded using a SpectraMax® i3x microplate reader with λ_{ex} 490 nm and λ_{em} 520 nm. Cellular metabolic activity was examined using the reduction of 3-(4,5-dimethylthiazol-2-yl)-5-(3-carboxymethoxyphenyl)-2-(4-sulfophenyl)-2H-tetrazolium (MTS assay) as described previously [16].

2.6. Statistics

GraphPad Prism was used for statistical analysis (version 6.07; GraphPad Software, San Diego, CA, USA). One-way ANOVA with Tukey's multiple comparison test was used to determine statistical differences, at the $p < 0.05$ level.

3. Results

3.1. Effects of MPO/H_2O_2/Cl^- and MPO/H_2O_2/SCN^- on human plasma fibronectin detected by ELISA

Human plasma fibronectin (0.02 μM) was exposed to MPO/H_2O_2/Cl^- and MPO/H_2O_2/SCN^- systems using both low (0.02 μM) and high (0.1 μM) concentrations of MPO to reflect a non-diseased and diseased state. Under the former conditions the molar ratio of MPO to fibronectin is 1:1, allowing stoichiometric binding [19] with an assumed single high affinity binding site. With the higher MPO concentration, binding to the fibronectin may occur at multiple sites, or result in non-bound enzyme being present. A range of H_2O_2 concentrations were examined (0, 20, 40, 80, 120, 160 μM). Physiological concentrations of Cl^- (100 mM) were used in the MPO/H_2O_2/Cl^- system, and either 20 μM or 500 μM SCN^- for the MPO/H_2O_2/SCN^- system. These two concentrations span the range of SCN^- detected in human plasma [36,38,42,43]. Structural modifications to the fibronectin protein were analyzed by ELISA, or by silver staining or immunoblotting, after protein separation by SDS-PAGE.

Incubation of human plasma fibronectin with MPO/H_2O_2/Cl^- resulted in a statistically-significant loss of recognition of the CBF epitope starting at an 800x molar excess of H_2O_2, with this occurring in a dose-dependent manner (Fig. 1A). A ~35% loss of epitope recognition was detected with the 1600x molar excess of H_2O_2 (Fig. 1A). No significant changes were detected with H_2O_2 alone (data not shown). Examination of the recognition of the HBF epitope showed a similar dose-dependent loss of recognition with a statistically-significant loss observed with the 800x molar excess of H_2O_2 and ~50% with the 1600x molar excess of H_2O_2 (Fig. 1B). Modifications to these epitopes were accompanied by a dose-dependent increase in epitopes recognized by

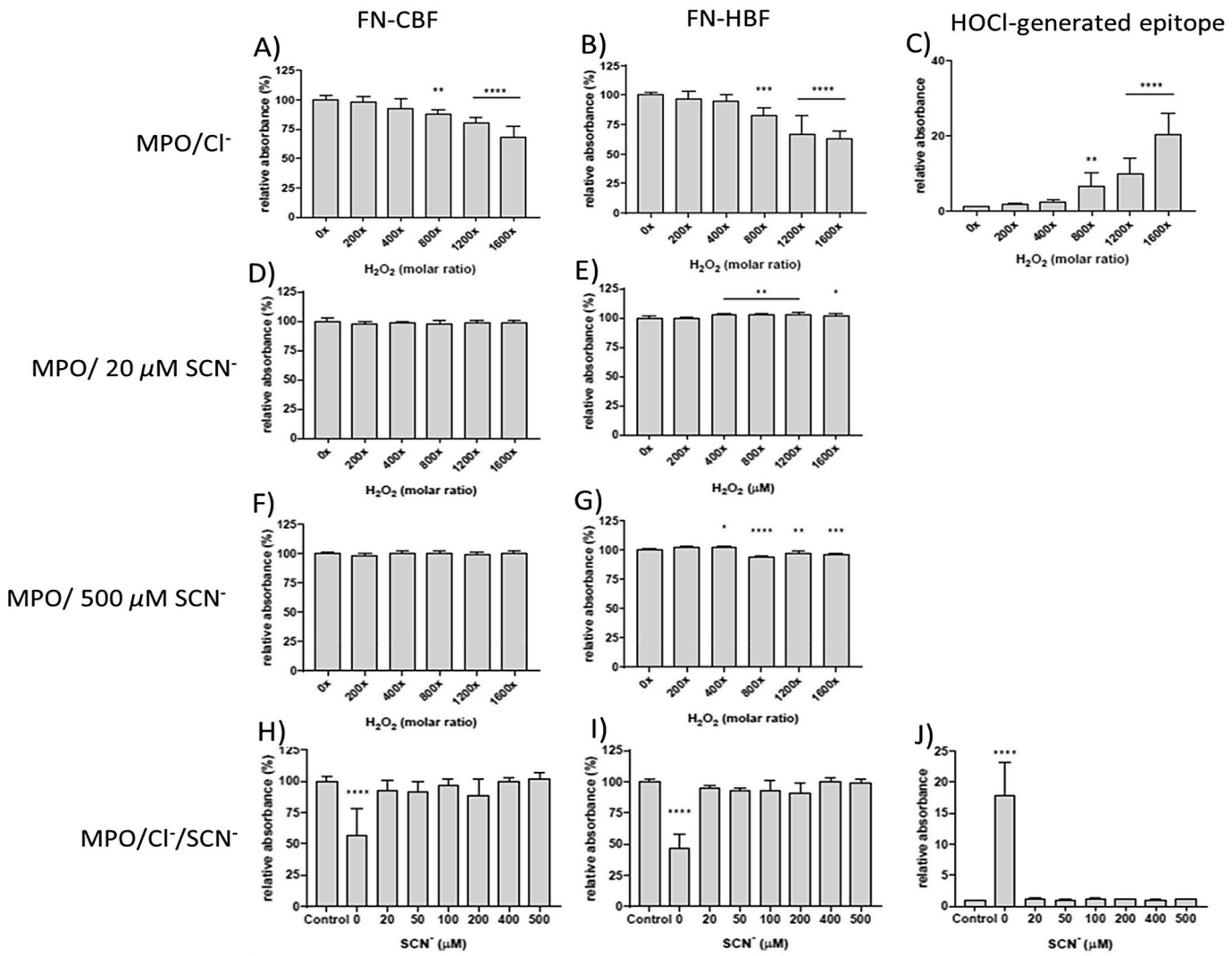

Fig. 1. ELISA of human plasma FN modified using enzymatic treatment with MPO/Cl^- or MPO/SCN^- in the presence of H_2O_2. Each well was coated with 0.5 μg (0.02 μM of FN in 0.1 M phosphate buffer, pH 7.4) and either left untreated (0 μM H_2O_2) or treated with 0.02 μM MPO/Cl^-, 0.02 μM MPO/20 or 500 μM SCN^-, 0.02 μM MPO/Cl^-/0–500 μM SCN^- and increasing concentrations of H_2O_2 (0, 4, 8, 16, 24, 32 μM), incubated for 2 h at 37 °C. FN epitopes were detected using a mouse monoclonal anti-FN CBF antibody (A17; 1:10000), anti-FN HBF antibody (A32; 1:1000), anti-HOCl generated epitope (2D10G9; 1:50), and conjugated with anti-mouse AP secondary (1:1000). The data are presented as a percentage relative to control (0 μM H_2O_2). Error bars are ±SD from three technical replicates obtained from each of three independent experiments. Statistical analysis was performed using one-way ANOVA with Tukey's multiple comparison post hoc tests to determine significance. Statistical significance is identified as follows: ** = $p < 0.01$, *** = $p < 0.001$, and **** = $p < 0.0001$.

mAb 2D10G9, an antibody raised against HOCl-damaged proteins (Fig. 1C). A statistically-significant increase in this material was detected with a 800x molar excess of H_2O_2, and further increases were detected with increasing H_2O_2 concentrations (Fig. 1C). These ELISA data mirror those observed with reagent HOCl [16].

Similar ELISA experiments were carried out with a MPO/SCN^-/H_2O_2 system using either 20 μM or 500 μM of SCN^- and identical concentrations of MPO and H_2O_2. Exposure of the fibronectin to 0.02 μM MPO with 20 μM of SCN^-, and up to a 1600x molar excess of H_2O_2, did not give any significant changes in CBF epitope recognition (Fig. 1D). However, with 500 μM SCN^- and increasing concentrations of H_2O_2 above a 400x molar excess, there was a statistically-significant increase in epitope recognition. This increase was sustained at higher H_2O_2 concentrations (Fig. 1E). Studies of the fibronectin HBF epitope, using 20 μM SCN^- and increasing concentrations of H_2O_2, provided no evidence for modifications to this epitope (Fig. 1F). With 500 μM SCN^-, and increasing molar excesses of H_2O_2, a small but significant increase in recognition of the HBF epitope was detected with a 400x molar excess of H_2O_2 (Fig. 1G), but with higher H_2O_2 concentrations (800x molar excess and up) this effect was reversed, and a significant loss of HBF epitope recognition was observed (Fig. 1G).

3.2. *Effects of MPO/H_2O_2/Cl^- and MPO/H_2O_2/SCN^- on human plasma fibronectin detected by SDS-PAGE with silver staining*

Fibronectin samples treated with an MPO enzymatic system with either 0.02 μM or 0.1 μM of MPO, 100 mM of Cl^-, and increasing concentrations of H_2O_2 (0, 20, 40, 80, 120, 160 μM), were analyzed by SDS-PAGE with silver staining (Fig. 2). As expected, for the untreated controls both the parent dimer (~440 kDa) and monomer (broad band at ~ 220 kDa with the two chains unresolved) were detected under non-reducing conditions, and only the monomer under reducing conditions, due to cleavage of the two inter-chain disulfide bonds. For enzyme treated samples, formation of dimers and higher aggregates (black arrow) were observed with both MPO concentrations, and under both non-reducing and reducing conditions. Increasing levels of aggregates were detected with increasing H_2O_2 concentrations, and the bands became more diffuse (smeared) at the highest oxidant levels, indicative

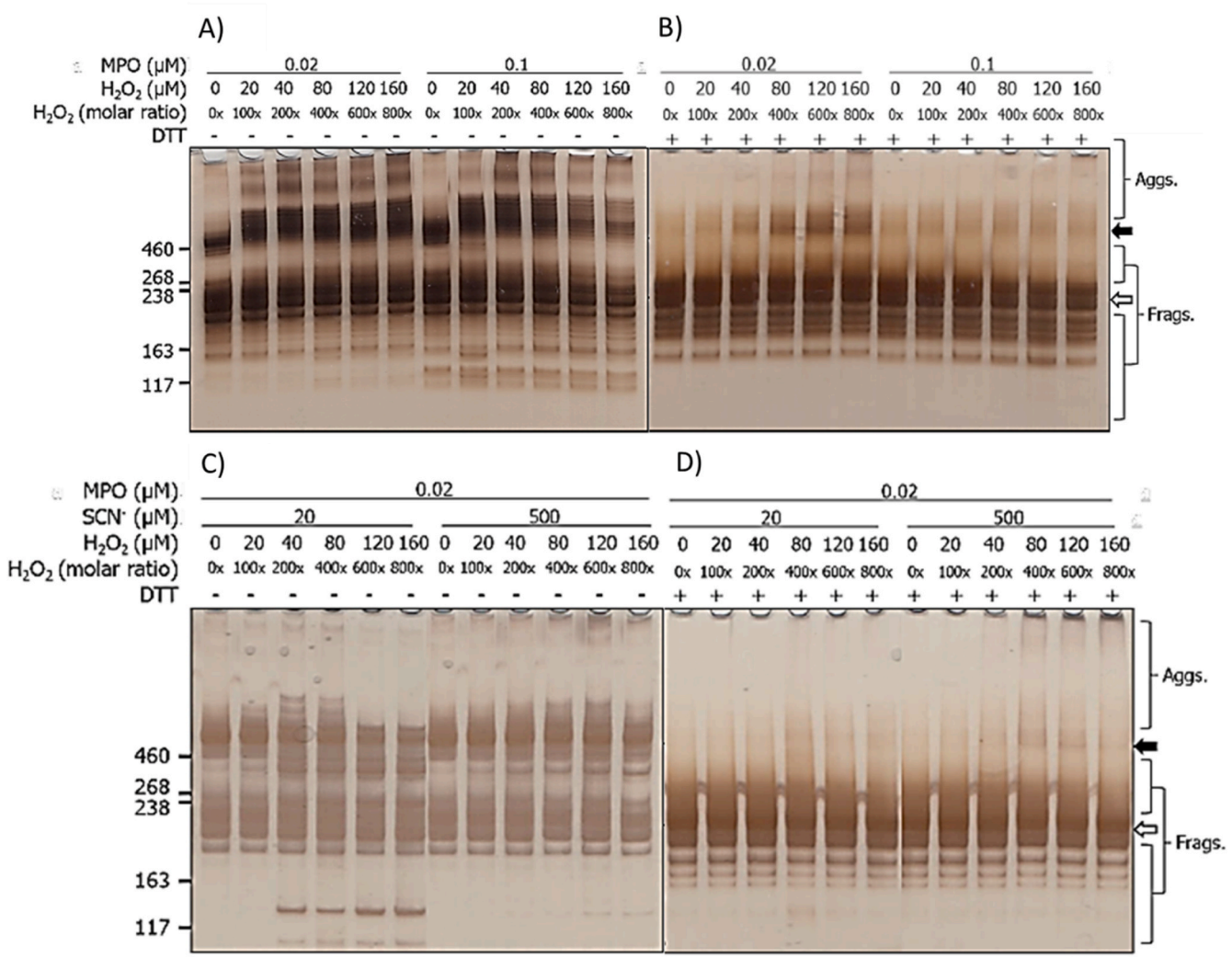

Fig. 2. Silver staining of SDS-PAGE gels indicates structural changes to human plasma FN treated with MPO/H_2O_2/Cl^- or MPO/H_2O_2/SCN^-. Purified human plasma FN (0.2 μM in 0.1 M phosphate buffer, pH 7.4) was left untreated (control 0x H_2O_2), treated with 0.02 or 0.1 μM MPO/Cl^- (A, B) or treated with 0.2 μM MPO/20 or 500 μM SCN^- (C, D) and increasing concentrations of H_2O_2 (0, 20, 40, 80, 120, 160 μM), and incubated for 2 h at 37 °C. Samples were electrophoresed on 3–8% Tris-acetate SDS-PAGE gels under non-reducing (A, C) or reducing conditions (B, D). Gels were then fixed, and visualized with silver staining and referenced against HiMark™ pre-stained High Molecular Mass standards. Data are labelled as follows: black arrow = dimer/higher aggregates, and white arrow = monomer bands.

of a heterogeneity in the species present. Concurrent with this, and with the higher concentration of MPO, a loss of the parent dimer (under non-reducing conditions, black arrow) and the monomer band (under both conditions, white arrow) were detected (Fig. 2). Bands assigned to species with altered structures were also detected, with both MPO concentrations, above and below the parent monomer, with higher oxidant exposure (Fig. 2). In addition, a shift in the apparent molecular mass of the dimer was detected in the presence of H_2O_2 compared to its absence (cf. the first two lanes in Fig. 2A). With the higher concentration of MPO, a prominent band was also detected at ~130 kDa, possibly from a fragment species; this was not detected with the lower concentration of MPO, or under reducing conditions.

For the samples run under reducing conditions, increasing concentrations of non-reducible dimers were detected with increasing concentrations of H_2O_2 (Fig. 2B), with this being particularly notable with the low MPO concentration. These species were less apparent with the higher MPO concentration (0.1 μM), but an increased amount of material was detected at the top of the gel, with high levels of H_2O_2, consistent with the presence of very high mass species, possibly formed by further reaction of initial oligomers (Fig. 2B). An increased abundance of species with altered mobility/structure was also detected with the 0.02 μM MPO treatment, just above the parent monomer band (Fig. 2B). These data suggest that the extent and/or types of modifications are dependent on the MPO concentration.

For the corresponding MPO/H_2O_2/SCN^- system, experiments were only carried out with the lower level of MPO (0.02 μM) and 0.02 μM fibronectin, but with either 20 μM or 500 μM of SCN^-, and increasing concentrations of H_2O_2. Under non-reducing conditions, with 20 μM SCN^-, increasing concentrations of H_2O_2 resulted in changes to the protein structure (Fig. 2C). With a 200-fold molar excess of H_2O_2, additional bands were detected above and below the dimer band at ~440 kDa. Higher mass bands (>460 kDa) decreased in intensity above a 400-fold excess of H_2O_2, whilst those with masses between 220 and 440 kDa were detected over the entire H_2O_2 concentration range examined (Fig. 2C). A prominent fragment was also detected at ~130 kDa, with the detection of this species being dependent on the presence and concentration of H_2O_2 (Fig. 2C). With 500 μM SCN^-, the species observed at masses above and below the dimer, with 20 μM SCN^-, were also detected, but the band at ~130 kDa was not observed (Fig. 2C). In addition, increased staining was detected at the top of the gels, and in the loading wells, with 200–800x molar excesses of H_2O_2 consistent with the presence of high mass aggregates (Fig. 2C). Under reducing conditions, less marked changes were detected, but low levels of non-reducible (covalent) cross-links were detected at ~440 kDa with

increasing H_2O_2 exposure, and higher levels of very high mass aggregates were detected near, and at, the top of the gels with high levels of H_2O_2 (Fig. 2D).

3.3. Effects of the MPO/H_2O_2/Cl^- and MPO/H_2O_2/SCN^- systems on human plasma fibronectin detected by SDS-PAGE with immunoblotting

Immunoblotting was used to examine potential changes to the CBF and HBF epitopes, using the same reactions systems described above. Immunoblots from non-reducing gels, probed with an anti-CBF mAb, showed a loss of antibody recognition in a H_2O_2 dose-dependent manner, with a marked loss observed with both MPO concentrations, and particularly 0.1 μM MPO, and 100–800x molar excesses of H_2O_2, with an appreciable loss in intensity of both the monomer (white arrow) and dimer (black arrow) bands (Fig. 3A). No significant changes were detected with H_2O_2 alone (data not shown). Aggregate formation was observed with both MPO concentrations, and particularly 0.02 μM MPO, with lower levels detected with the high MPO concentration (Fig. 3A). Under reducing conditions, the loss of the monomer band immunoreactivity was less noticeable with both MPO concentrations, but a notable formation of covalent (non-reducible) dimers with apparent masses > 460 kDa, were detected with both MPO concentrations, and particularly low MPO levels. These data are consistent with different behavior of the two MPO concentrations (Fig. 3B). Similar experiments with the HBF mAb yielded a similar pattern of changes with blots run under both non-reducing and reducing conditions (Fig. 3C and D respectively), with formation of species with altered gel mobility, generation of reducible and non-reducible dimers and aggregates, and a loss of parent protein recognition, particularly with the higher concentration of MPO and high H_2O_2. Experiments were not carried out with mAb 2D10G9, as this antibody does not work effectively in immunoblotting [16].

Analogous experiments were carried out with the MPO/SCN^-/H_2O_2 system (as above). The changes detected to the fibronectin CBF under non-reducing conditions were similar to those detected at the protein level by silver staining (Fig. 2A), though more pronounced. With 20 μM SCN^-, and H_2O_2 molar excesses ≥200, a significant loss of antibody recognition of both the parent dimer and monomer bands were detected, which was dose-dependent with higher H_2O_2 concentrations (Fig. 4A). In addition, formation of a prominent fragments, containing the CBF domain, with an apparent molecular mass of 300–350 kDa (i.e. between the parent dimer and monomer bands) was observed (Fig. 4A). With 500 μM SCN^- a similar, but less marked (when compared to 20 μM SCN^-) loss of recognition of the parent dimer and monomer bands was detected (Fig. 4A). Fragmentation to give the 300–350 kDa species was also detected but to a lesser extent (Fig. 4A). Under reducing conditions, a minor loss of anti-CBF recognition against the parent monomer band was detected with both concentrations of SCN^- (Fig. 4B), the 300–350 kDa fragment was not observed, but low levels of dimers with a mass of ~460 kDa were detected with increasing H_2O_2 concentrations (Fig. 4B). The anti-HBF antibody gave a similar pattern of data (Fig. 4C and D). For

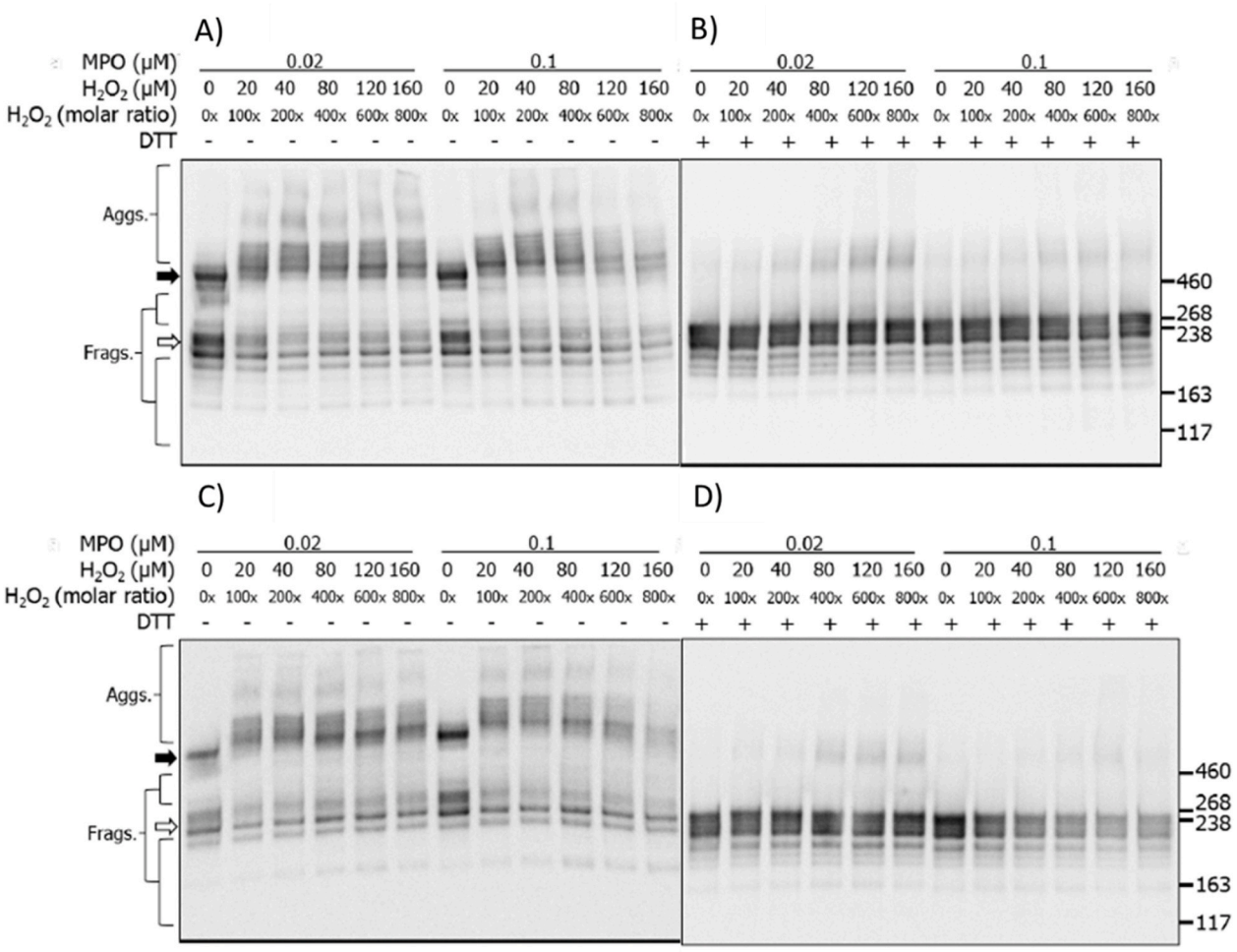

Fig. 3. Immunoblots of structural changes to human plasma fibronectin treated with MPO/H_2O_2/Cl^-. Samples were separated on SDS-PAGE under non-reducing (A, C) or reducing (B, D) conditions as described in the legend to Fig. 2, and then transferred onto PVDF membranes and probed with mouse monoclonal anti-FN CBF antibody (A, B; A17; 1:10000) or anti-FN HBF antibody (C, D; A32; 1:2000), followed by anti-mouse HRP-conjugated secondary antibody (1:2000). Blots were developed with chemiluminescence reagent and data labelled as follows: black arrow = dimer/higher aggregates, and white arrow = monomer bands.

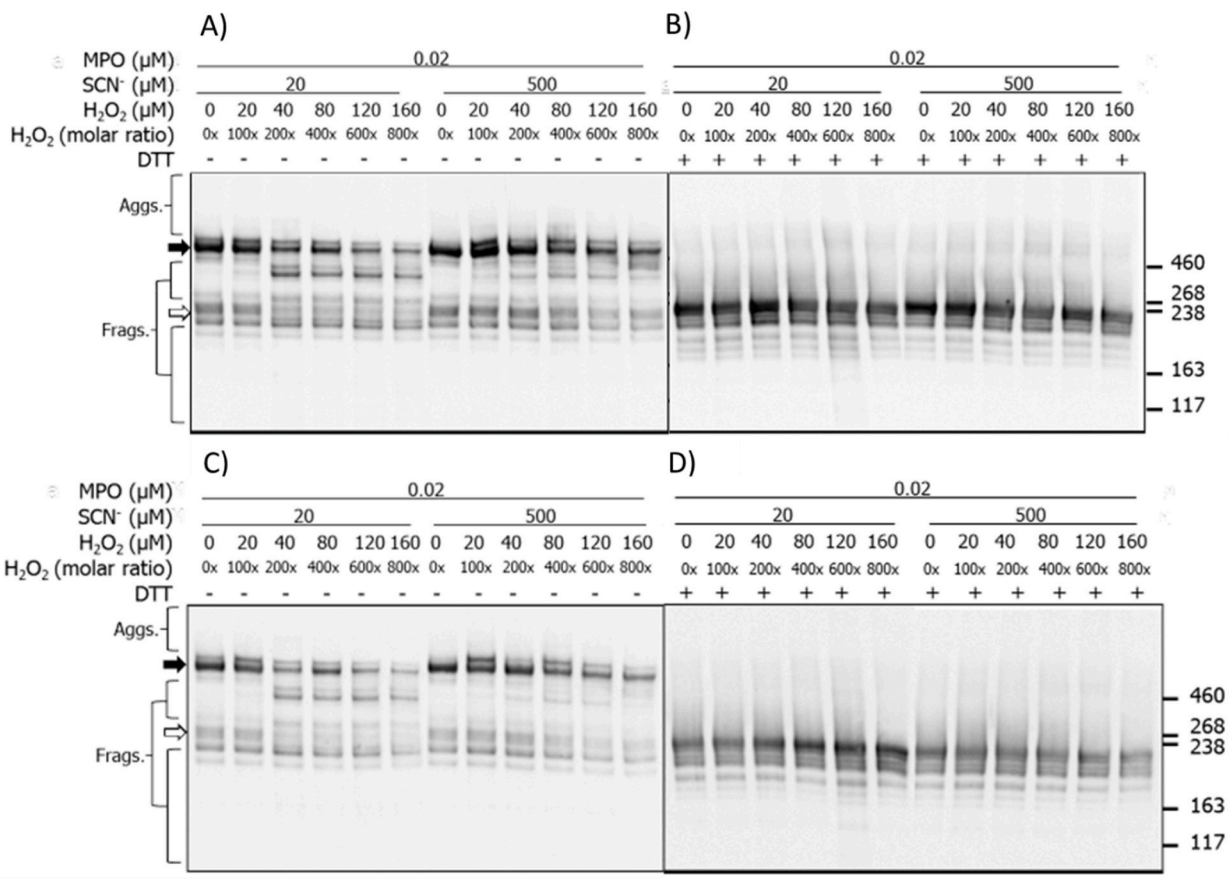

Fig. 4. Immunoblots of structural changes to human plasma FN treated with MPO/H_2O_2/SCN^-. Human plasma FN was separated using SDS-PAGE under non-reducing (A, C) or reducing (B, D) conditions, and then transferred onto PVDF membranes and probed with either the mouse monoclonal anti-FN CBF antibody (A, B; A17; 1:10000) or anti-FN HBF antibody (C, D; A32; 1:2000), followed by HRP conjugated anti-mouse HRP secondary antibody (1:2000). Blots were developed with chemiluminescence reagent and data labelled as follows: black arrow = dimer/higher aggregates, and white arrow = monomer band.

gels run under non-reducing conditions, with both 20 μM and 500 μM SCN^-, a dose-dependent loss of recognition of both the parent dimer and monomer bands were detected with 200–800x molar excesses of H_2O_2 (Fig. 4C), and the fragment species at 300–350 kDa was detected with a 200x molar excess, or higher, of H_2O_2; this fragment was less prominent at higher SCN^- concentration (Fig. 4C). For the samples electrophoresed under reducing conditions less marked changes were detected, though with 20 μM SCN^-, an increased recognition of the HBF was detected with increasing concentrations of H_2O_2 (Fig. 4D). This was less apparent with 500 μM SCN^- (Fig. 4D). Neither fragmentation nor crosslink formation was observed for either low or high concentrations of SCN^- under reducing conditions (Fig. 4D).

In light of these data indicating modifications to the biologically important CBF of fibronectin, experiments were performed to quantify human coronary artery endothelial cell (HCAEC) adhesion and metabolic activity on exposure to modified fibronectin.

3.4. Effects of the MPO/H_2O_2/Cl^- and MPO/H_2O_2/SCN^- induced modification on human plasma fibronectin on primary human coronary artery endothelial cell (HCAEC) adhesion and metabolic activity

Surface-bound human plasma fibronectin (0.02 μM) was left untreated (control) or treated with the MPO/H_2O_2/Cl^- system using either 400- or 1600-fold molar excesses of H_2O_2; the full range of H_2O_2 concentrations used in the SDS-PAGE and immunoblotting studies were not employed due to the low availability of primary human cells. Fibronectin that had been oxidant-treated was washed twice to remove excess oxidant before addition of the cells, thereby preventing direct cell-oxidant interactions. Pre-treatment of fibronectin with MPO/H_2O_2/Cl^-, with increasing concentrations of H_2O_2, prior to cell addition resulted in a statistically-significant (~30%) loss of HCAEC adhesion with a 1600x molar excess of H_2O_2, when compared to untreated controls (0x H_2O_2 molar excess; Fig. 5A). As cells may remain attached to a sub-strata, but have reduced metabolic activity, studies were also carried out to assess functional activity on exposure to modified fibronectin. Thus, HCAEC adherent on native and modified fibronectin (as above) were subsequently incubated in growth media for a further 48 h. MTS reagent was then added, and reduction of MTS to formazan by cellular NAD(P)H dehydrogenase enzymes was quantified. Cells incubated on fibronectin pre-treated with MPO/H_2O_2/Cl^- using a 400x or 1600x molar excess of H_2O_2, showed a statistically-significant decrease in metabolic activity (Fig. 5D). The corresponding MPO/H_2O_2/SCN^-system with either 20 μM or 500 μM SCN^-, and a 400x or 1600x molar excesses of H_2O_2, did not give any statistically-significant differences in HCAEC adhesion (Fig. 5B and C) or metabolic activity (Fig. 5E and F). In light of these differences between the MPO/H_2O_2/Cl^- and MPO/H_2O_2/SCN^- systems, investigations were conducted with a MPO/H_2O_2/Cl^-/SCN^- systems with Cl^- and SCN^- present simultaneously but at different ratios.

3.5. Effects of MPO/H_2O_2/Cl^- systems in the presence of increasing concentrations of SCN^- on functional epitopes of human plasma fibronectin detected by ELISA

Surface-bound human plasma fibronectin (0.02 μM) was incubated with MPO (0.02 μM), Cl^- (100 mM), SCN^- (0–500 μM) and H_2O_2 (32

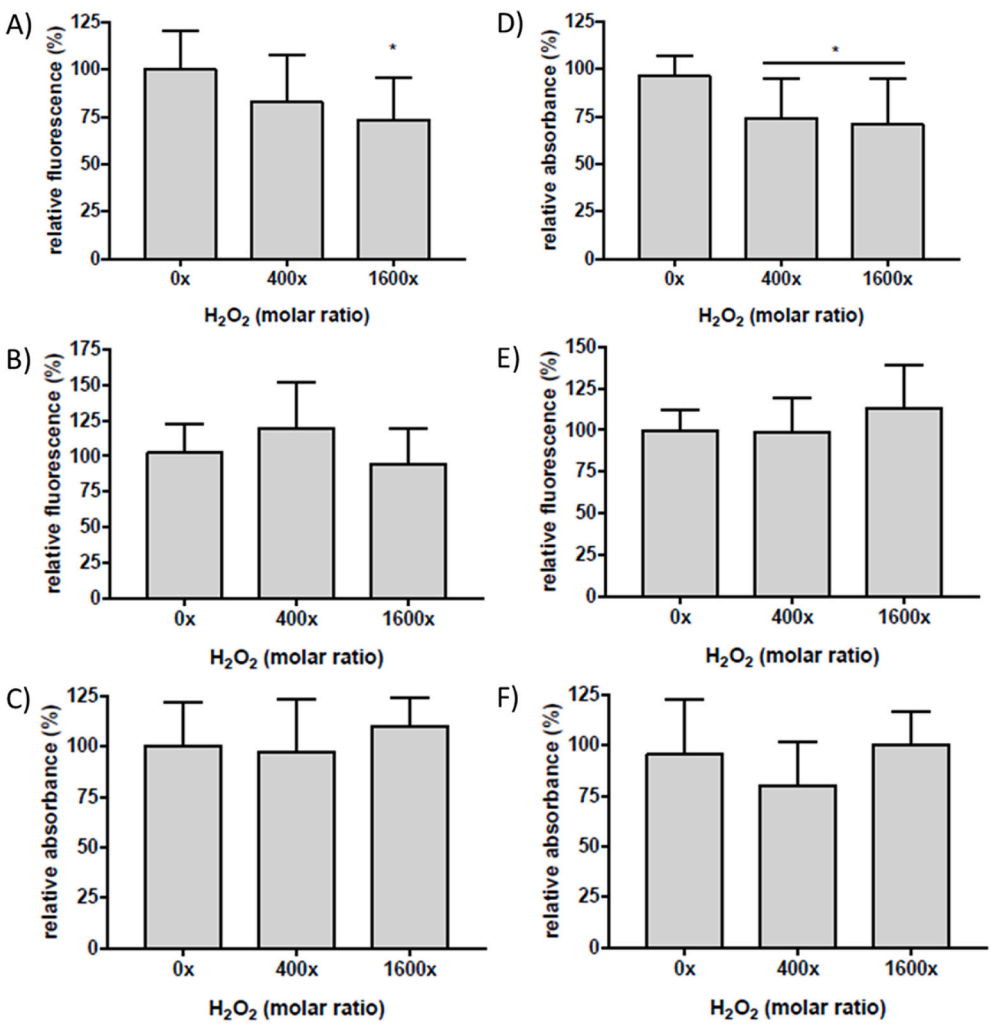

Fig. 5. Calcein-AM fluorescence and proliferation of HCAEC incubated on human plasma FN treated with MPO/H_2O_2/Cl^- or MPO/H_2O_2/SCN^-. Surface-bound human plasma FN (0.02 μM) was left untreated (0x H_2O_2), treated with MPO/Cl^- (A, D), MPO/20 μM SCN^- (B, E) or MPO/500 μM SCN^- (C, F), and increasing concentration of H_2O_2 (0, 8, 32 μM) and incubated for 2 h at 37 °C before incubation with HCAEC pre-stained with calcein-AM and subsequent detection of fluorescence to quantify cell adhesion (A, B, C). Plates were then washed prior to addition of growth media and HCAEC were left to recover over 48 h. MTS reagent was added into each well and absorbance was measured at 490 nm after 3 h for cell proliferation assay (D, E, F). All data are presented as a percentage of the control, with no added H_2O_2. Error bars are ±SD from three technical replicates obtained from each of three independent experiments. Statistical analysis was performed using one-way ANOVA with Tukey's multiple comparison post hoc tests to determine significance. Statistical significance is identified as follow: * = $p < 0.05$.

μM, i.e. 1600-fold molar excess, added last) for 2 h at 37 °C. The wells were then washed before analysis by ELISA for CBF and HBF epitopes, and material recognized by mAb 2D10G9. Treatment in the absence of added SCN^- resulted in a significant loss in recognition of the CBF and HBF epitopes, and a significant increase in material recognized by 2D10G9 (Fig. 1H–J, cf. Fig. 1A–C). However, the presence of 20 μM or higher SCN^- reversed these changes, with the absorbance values restored to control levels (Fig. 1H–J).

3.6. *Effects of MPO/H_2O_2/Cl^- with increasing concentrations of SCN^- on functional epitopes of human plasma fibronectin detected by SDS-PAGE-silver staining and immunoblotting*

The effects of increasing SCN^- on the structural changes induced by the MPO/H_2O_2/Cl^- system were examined by SDS-PAGE with silver staining, and also by immunoblotting. Purified human plasma fibronectin (0.02 μM) was either left unoxidized (MPO only control) or treated with MPO (0.02 or 0.1 μM), Cl^- (100 mM), SCN^- (0–500 μM) and H_2O_2 (160 μM, added last). Samples were then separated on SDS-PAGE prior to silver staining or immunoblotting. Under non-reducing conditions, the fibronectin monomer bands (white arrow) were decreased in staining intensity by MPO/H_2O_2/Cl^- treatment in the absence of SCN^- (Fig. 6A). This treatment also induced fragmentation, with additional bands detected at lower molecular masses, and aggregates at higher molecular mass. In the presence of 20 μM SCN^-, fewer higher mass aggregates were detected, but greater staining intensity between 260 and 460 kDa, suggesting that these phenomena are linked (Fig. 6A). Additional fragments with masses <190 kDa were more prominent with increasing concentrations of SCN^- (Fig. 6A). With high concentrations of SCN^- (400 and 500 μM), fewer bands were detected in the 260–460 kDa range, and the intensity of the lower mass fragments was reduced. Experiments carried out with 0.1 μM MPO under non-reducing conditions, gave similar modifications to those seen with 0.02 μM MPO, together with greater loss of the parent dimer (black arrow) and monomer bands (white arrow) (Fig. 6A). In the presence of 500 μM SCN^-, the modifications detected were similar to those detected with the MPO/H_2O_2/SCN^- system (Fig. 2C), and pre-formed HOSCN [16].

Similar samples run under reducing conditions, indicated the presence of the fibronectin monomer and fragments in the absence of SCN^- with both MPO concentrations (Fig. 6B). These species were also detected in the presence of SCN^- at concentrations up to 100 μM, but at higher SCN^- concentrations these species were less prevalent and almost completely absent at the highest concentrations (Fig. 6B). With the higher SCN^- concentrations, low levels of non-reducible dimers were detected together with some smearing of the monomer band to higher apparent masses (Fig. 6B).

Immunoblotting for the CBF and HBF epitopes was also employed, as described above. Under non-reducing conditions, use of the anti-CBF antibody, in the absence of SCN^-, showed the presence of extensive aggregation and fragmentation, together with a loss of the parent monomer (white arrow) and dimer bands (black arrow) (Fig. 7A; cf. Fig. 3). In the presence of added SCN^- (20 μM) several specific fragments were detected, with masses between those of the dimer and

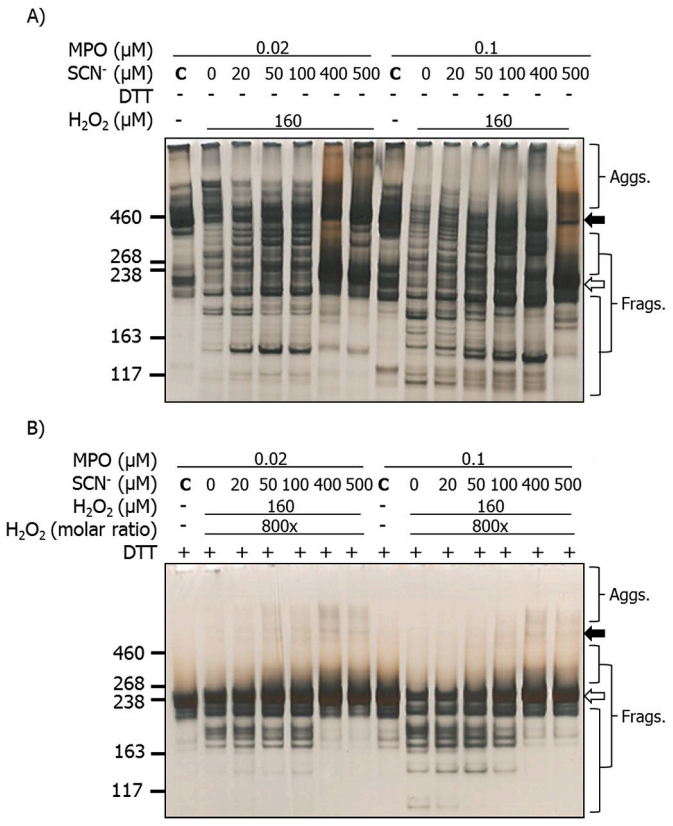

Fig. 6. Silver staining of SDS-PAGE gels showing structural changes to human plasma FN treated with MPO/H_2O_2/Cl^- in the presence of increasing concentrations of SCN^-. Purified human plasma FN (0.2 μM in 0.1 M phosphate buffer, pH 7.4) was either left untreated (MPO only control) or treated with MPO/H_2O_2/Cl^- and the indicated concentrations of SCN^- for 2 h at 37 °C. Samples were electrophoresed using 3–8% Tris-acetate SDS-PAGE gels under: A) non-reducing, or B) reducing conditions. Gels were then fixed, and visualized with silver staining and referenced against HiMark™ pre-stained high molecular mass standards. Black arrow = dimer/higher aggregates; white arrow = monomer bands.

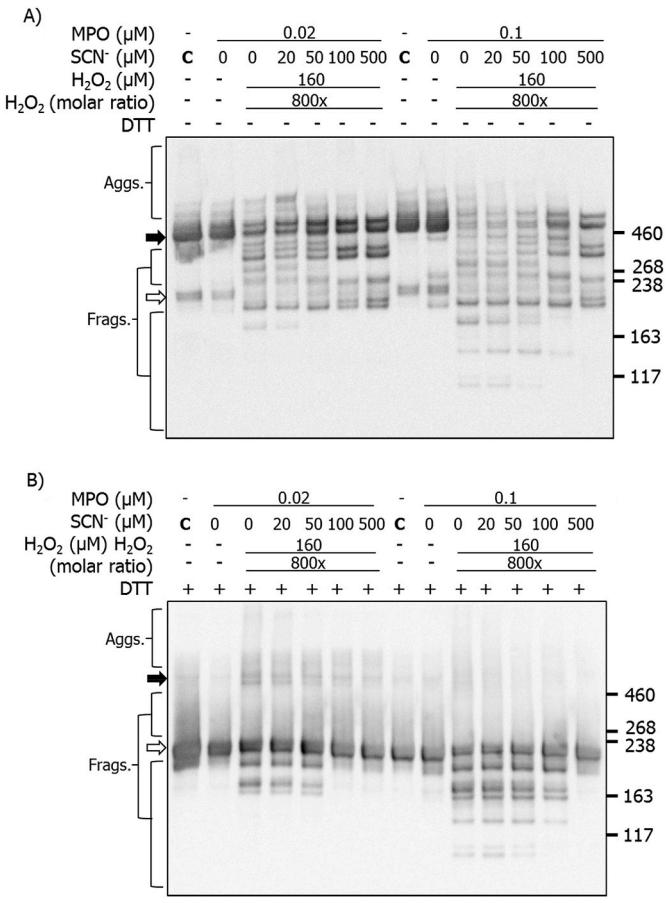

Fig. 7. Immunoblotting for CBF showing structural changes to human plasma FN treated with a MPO/H_2O_2/Cl^- system in the presence of increasing concentrations of SCN^-. Purified human plasma FN (0.2 μM in 0.1 M phosphate buffer, pH 7.4) was either left untreated (MPO only control) or treated with MPO (0.02 or 0.1 μM), Cl^- (100 mM), H_2O_2 (160 μM) and increasing concentration of SCN^-, and incubated for 2 h at 37 °C. Samples were electrophoresed on SDS-PAGE under A) non-reducing or B) reducing conditions, transferred onto PVDF membranes and probed with a mouse monoclonal anti-FN CBF antibody (A17; 1:10000), and conjugated with anti-mouse HRP secondary antibody (1:2000). Blots were developed with ECL-plus reagent. Black arrow = dimer/higher aggregates; white arrow = monomer bands.

monomer (Fig. 7A). Increases in the SCN^- concentration led to a decrease in HOCl-induced modifications, with the detection of fragments and aggregates similar to those seen with the MPO/H_2O_2/SCN^- system with no Cl^- (cf. Fig. 4A). Of particular note is the recovery of recognition of the parent fibronectin band with high SCN^- levels, consistent with decreased modification of the parent protein, though the appearance of two discreet bands suggests two populations of the dimeric protein are present. Similar, but more marked effects were detected in experiments carried out using 0.1 μM MPO.

Analogous experiments carried out under reducing conditions (Fig. 7B), yielded data indicating that increasing concentrations of SCN^- decrease the extent of modification induced by MPO-generated HOCl. Thus, with both concentrations of MPO, in the presence of H_2O_2 and Cl^-, significant formation of both non-reducible (covalent) dimers and also fragments were detected. However, the presence of increasing concentrations of SCN^- decreased this damage, such that with the highest levels of SCN^-, HOCl-mediated modification was almost completely abrogated (Fig. 7B). Similar behavior was detected for both the non-reducing and reducing system when the membranes were probed with the anti-HBF antibody (Fig. 8A and B).

4. Discussion

The experiments reported here indicate the exposure of fibronectin to an enzymatic MPO/H_2O_2/Cl^- system results in damage to the functionally important CBF and HBF domains and gross structural changes to the protein. These changes result in altered adhesion and metabolic activity of naïve HCAEC exposed to this pre-oxidized fibronectin. Significant differences were observed between the effects of stoichiometric, and above-stoichiometric, MPO relative to the fibronectin concentration, consistent with stoichiometric binding of MPO to fibronectin. In contrast, the MPO/H_2O_2/SCN^- system induced limited changes, with no damage detected to the CBF and HBF domains, less protein modification, and no effects on HCAEC adhesion or metabolic activity. Addition of increasing SCN^- to the MPO/H_2O_2/Cl^- system, to provide competition for the key MPO catalytic intermediate and therefore decrease HOCl formation, afforded protection, with >20 μM SCN^- decreasing damage to the functional domains and protein structure, and maintaining native HCAEC behavior.

High plasma MPO levels are associated with an elevated incidence of cardiovascular pathologies, and are both diagnostic of disease, and prognostic of poor outcomes (e.g. Ref. [44–47]). MPO may accumulate in the sub-endothelial space of the artery wall as a result of extracellular release from leukocytes as a consequence of inappropriate cellular processing, phagolysosomal leakage, and cell damage/death (e.g. NETosis or necrosis), or as a result of ingress from plasma, as MPO

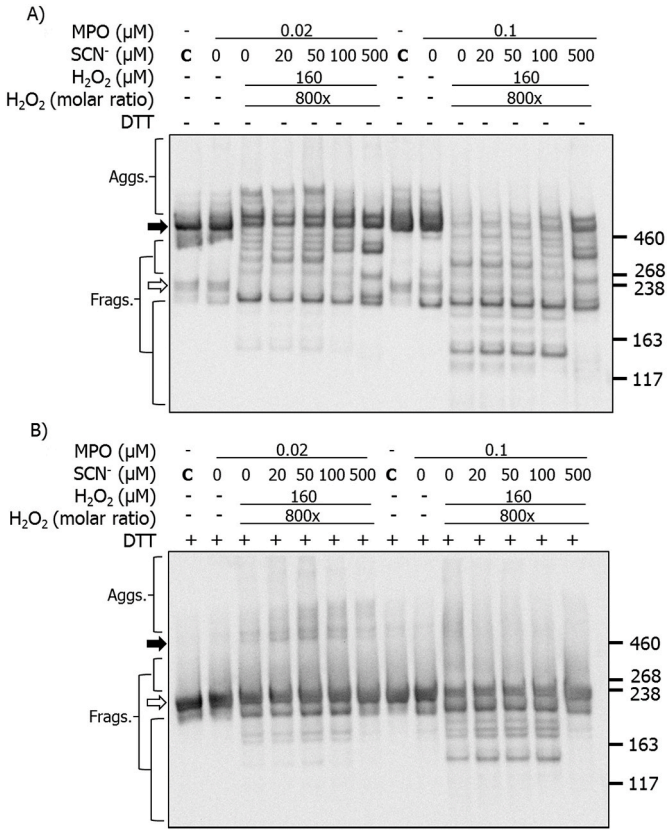

Fig. 8. Immunoblotting for HBF showing structural changes to human plasma FN treated with a MPO/H_2O_2/Cl^- system and increasing concentrations of SCN^-. Purified human plasma FN (0.2 μM in 0.1 M phosphate buffer, pH 7.4) was either left untreated (MPO only control) or treated with MPO (0.02 or 0.1 μM), Cl^- (100 mM), H_2O_2 (160 μM) and increasing concentration of SCN^-, and incubated for 2 h at 37 °C. Samples were electrophoresed on SDS-PAGE under A) non-reducing or B) reducing conditions, transferred onto PVDF membranes and probed with a mouse monoclonal anti-FN HBF antibody (A32; 1:5000), and conjugated with anti-mouse HRP secondary antibody (1:2000). Blots were developed with ECL-plus reagent. Black arrow = dimer/higher aggregates; white arrow = monomer band.

undergoes rapid transcytosis through endothelial cells [25,48,49]. MPO binds to extracellular materials including low- and high-density lipoproteins [50–53], glycosaminoglycans, proteins, proteoglycans and glycoproteins of the ECM [19,23,25,54–56], via ionic interactions, resulting from the cationic nature of MPO (pI 9.2). The bound MPO appears (at least in some cases) to be catalytically-active [19], and capable of inducing the formation of di-Tyr [57,58], carbonyl compounds [19,59], and biological dysfunction [17,19,23,60]. High levels of fibronectin are present in human atherosclerotic lesions [26,27], and co-localization of MPO, HOCl-modified proteins, and macrophages has been observed in atherosclerotic lesions [61]. The accumulation of fibronectin during atherogenesis may drive MPO accumulation, and contribute to MPO-mediated damage in the growing lesion, as HOCl would be expected to react with nearby species due to its high reactivity with proteins [62–64] and limited diffusion radius [65]. Thus, both fibronectin and MPO have been reported to be targets of HOCl [17]. Previous MS studies have mapped the type and extent of these modifications [16,17]. Interestingly, the extent of MPO binding appears to increase with higher levels of fibronectin modification [19], consistent with a vicious cycle of binding, catalytic activity, fibronectin damage and further MPO binding [19].

Analysis of the effects of MPO/H_2O_2/Cl^- system on human plasma fibronectin indicate that aggregate formation occurs with low (100x) molar ratios of H_2O_2 (Fig. 2). This was observed under both reducing and non-reducing conditions, with higher levels detected in the latter case, consistent with both reducible (probably disulfide) and non-reducible crosslinks. This behavior is similar to that of reagent HOCl under identical conditions [16]. The reducible aggregates are therefore ascribed to HOCl reactions, rather than inter-protein electron transfer processes [66], or MPO-derived radicals [67]. A plausible mechanism involves conversion of Cys residues, by HOCl [68], to sulfenic acids (RSOH) that then react with another thiol to form a disulfide [69]. This may occur intra-, or inter-molecularly to give reducible cross-linked species [70]. This mechanism is supported by the known consumption of Cys residues on fibronectin by reagent HOCl [16]. The non-reducible cross-links (Fig. 2) may involve inter-molecular di-Tyr, di-Trp, Trp-Tyr, or other linkages which contain strong covalent bonds [71], formed by radical-radical dimerization (e.g. of two Tyr phenoxyl radicals, two Trp-indolyl radicals, or cross-reactions of these species [71,72]). Di-Tyr has been reported on fibronectin exposed to an MPO system, and in greater quantities than with reagent HOCl [59]. These data implicate radical intermediates, possibly generated by electron transfer from fibronectin to Compound I or II of MPO (cf. data for other heme proteins and peroxidases [66,67,73]).

The fibronectin fragmentation detected with MPO/H_2O_2/Cl^- (Fig. 2) is similar to that detected with reagent HOCl [16], and increased with higher concentrations of H_2O_2. This fragmentation may arise via (non-radical) chloramine/chloramide formation and subsequent hydrolysis reactions to give carbonyls [74–76], or via nitrogen-centred radicals formed on chloramine/chloramide decomposition; both processes are known to result in protein fragmentation [74,75].

Apparent shifts in molecular mass were observed for fibronectin exposed to MPO/H_2O_2/Cl^- (Fig. 2). These only occurred in the presence of H_2O_2, and hence are not a result of direct MPO binding, and therefore are likely to arise from oxidant-induced reactions. HOCl can modify specific protein side chains, resulting in unfolding or altered protein conformations, that migrate differently on gels, and thereby appear to have an altered molecular mass [16,77]. Oxidation can also increase the molecular mass of proteins as a result of (multiple) oxygen or chlorine atom incorporation [78], but the apparent mass changes are large, and hence unlikely to arise from this mechanism. Further investigations are needed to define the origin of these changes, which may be highly heterogenous.

The differences observed between the low (0.02 μM) and high MPO (0.1 μM) concentrations in the MPO/H_2O_2/Cl^- system (cf. Figs. 2B and 3A and B), is consistent with MPO binding to fibronectin (as reported previously [19]), with more marked alterations seen with stoichiometric concentrations, than when the MPO is at higher concentrations. This may be due to binding of excess MPO to other fibronectin sites, or the presence of unbound MPO which generates oxidants in free solution, and leads to untargeted protein damage.

HOSCN is a major alternative oxidant generated by the MPO system when SCN^- is present in the absence of Cl^-, or when concentrations of SCN^- are towards the higher end of the concentrations detected physiologically in humans (see earlier) in the presence of Cl^-. Treatment of fibronectin with MPO/SCN^- and increasing amounts of H_2O_2 (Fig. 3) resulted in structural modifications similar to those observed with reagent HOSCN [16]. As HOSCN has a high specificity for thiols [31], these aggregates are likely to be disulfide-linked species, formed from the limited number of Cys residues in fibronectin, or from oxidant-catalyzed thiol-disulfide exchange [79]. This conclusion is supported by the Cys depletion observed with reagent HOSCN [16], which is greater than that observed with HOCl. The apparent changes in fibronectin molecular mass is likely to arise, in this case, from modified protein conformers, rather than backbone cleavage, as there are limited data for HOSCN-induced fragmentation [31,80].

Localized damage induced by MPO/H_2O_2 arising from MPO bound to fibronectin, may explain the epitope changes observed in the presence of Cl^- or SCN^-. However, as a complete 3-D structure of fibronectin is not available, and putative MPO binding site(s) are unknown, the

modification data available for HOCl and MPO/H_2O_2/Cl^- cannot be fully interpreted [17]. However, despite this, the *consequences* are relatively clear. Fibronectin typically promotes endothelial cell proliferation [81–84], probably via multiple mechanisms, including cell shape modulation, interactions involving cell-surface integrins, PI3 kinase and NF-kappa B pathways, and mTOR signaling [81–84]. However, modification of fibronectin by MPO/H_2O_2/Cl^- results in decreased adhesion and 'rounding up' of human umbilical vein [22] and bovine aortic endothelial cells [23]. In the latter case, this has been attributed to an inability of cells to bind to modified ECM via an F-actin mediated adhesion pathway [23]. The data presented here (and also previously with reagent HOCl [16]), indicate that adhesion and metabolic activity of primary HCAEC are impaired when fibronectin is modified prior to HCAEC addition. The experimental design employed here does not involve any direct oxidant exposure of the cells, and therefore indicates that the protein modifications are causal in these changes. The reduction in CBF and HBF recognition that are important for cell binding (Figs. 1 and 3) are consistent with this loss of adhesion (Fig. 5), as is the increased recognition of fibronectin by mAb 2D10G9, which is indicative of HOCl-mediated damage. In contrast, the MPO/H_2O_2/SCN^- system induced only modest CBF changes, with these being less severe than with reagent HOCl and HOSCN [16], and also MPO-derived HOCl. Both reagent HOSCN [16] and MPO-derived HOSCN (Fig. 3) had little effect on the HBF epitope. Consistent with these data, no changes were detected in HCAEC cell adhesion and metabolic activity.

The Cl^- and SCN^- concentrations present *in vivo* determine the relative concentrations of HOCl and HOSCN generated by MPO. HOCl can also react directly with SCN^- (k 2.3 × 10^7 M^{-1} s^{-1} [85]) further diminishing HOCl, and enhancing HOSCN, levels. Consistent with these data, increasing concentrations of SCN^- modulated the effects of the MPO/H_2O_2/Cl^- system, with 20 μM SCN^- giving a complete reversal of the loss of CBF and HBF recognition, as detected by ELISA, and disappearance of the HOCl-generated epitopes recognized by 2D10G9 (Fig. 1). This suggests that these conditions minimize HOCl formation.

In contrast to the ELISA data, some limited modifications were detected with high concentrations of SCN^- on the SDS-PAGE gels and immunoblots, though concentrations >100 μM did decrease fragmentation and aggregation. The differences between the ELISA and SDS-PAGE data are likely to be due to the higher H_2O_2 concentrations used for the experiments (though the SCN^-: H_2O_2 *ratio* was kept constant) and hence a greater oxidant flux. The modifications detected with the highest concentrations of SCN^-, suggest that MPO-derived HOSCN can induce modifications, probably at Cys residues, but these do not impact on the CBF or HBF domains significantly (cf. the ELISA data). Thus, HOSCN does appear to modify fibronectin to a limited extent, but in a different manner to HOCl or MPO/H_2O_2/Cl^-.

Overall, the data presented here support the hypothesis that MPO, in the presence of H_2O_2 and Cl^- or SCN^-, generates HOCl and HOSCN (respectively), and also radicals, that modify fibronectin by different mechanisms. Cl^- and SCN^- appear to compete for reaction with Compound I of MPO, with increasing concentrations of SCN^- decreasing: a) HOCl generation; b) the extent of functionally-important (but not all) modifications on fibronectin; and c) the loss in endothelial cell adhesion and metabolic activity. The enzyme system with both anions present, is likely to mimic the situation *in vivo* more closely than the reagent oxidants, or either enzyme system *per se*. Furthermore, interactions between MPO and fibronectin appear to modulate both the sites and severity of damage, with the modifications induced by stoichiometric (or less) MPO, relative to fibronectin, showing greater differences to the reagent oxidant, than the high MPO system, consistent with MPO binding directing damage to particular sites. These sub-stoichiometric or stoichiometric systems are most likely to be of biological relevance. Enhancing SCN^- levels at *in vivo* sites of inflammation, where MPO induces tissue damage, should induce a switchover from HOCl to HOSCN formation, limit tissue modification and be of potential therapeutic value, as suggested by *in vitro* and *in vivo* studies [35–37,39].

Declaration of competing interest

The authors declare no conflicts of interest with regard to the data presented.

Acknowledgements

The authors are grateful to the Novo Nordisk Foundation (Laureate Research Grant NNF13OC0004294 to MJD), and the Danish Council for Independent Research | Natural Sciences (grant: DFF-7014-00047 to MJD) for financial support of these studies. SV thanks the Australian Government for a PhD scholarship. Prof. Ernst Malle is thanked for the providing the 2D10G9 antibody, and Dr. Huan Cai for valuable scientific discussions.

References

[1] M.J. Davies, C.L. Hawkins, The role of myeloperoxidase (MPO) in biomolecule modification, chronic inflammation and disease, Antioxidants Redox Signal. 32 (2020) 957–981.
[2] S.J. Klebanoff, A.J. Kettle, H. Rosen, C.C. Winterbourn, W.M. Nauseef, Myeloperoxidase: a front-line defender against phagocytosed microorganisms, J. Leukoc. Biol. 93 (2013) 185–198.
[3] M.J. Davies, C.L. Hawkins, D.I. Pattison, M.D. Rees, Mammalian heme peroxidases: from molecular mechanisms to health implications, Antioxidants Redox Signal. 10 (2008) 1199–1234.
[4] C.J. van Dalen, M.W. Whitehouse, C.C. Winterbourn, A.J. Kettle, Thiocyanate and chloride as competing substrates for myeloperoxidase, Biochem. J. 327 (1997) 487–492.
[5] P.G. Furtmuller, M. Zederbauer, W. Jantschko, J. Helm, M. Bogner, C. Jakopitsch, C. Obinger, Active site structure and catalytic mechanisms of human peroxidases, Arch. Biochem. Biophys. 445 (2006) 199–213.
[6] V. Papayannopoulos, K.D. Metzler, A. Hakkim, A. Zychlinsky, Neutrophil elastase and myeloperoxidase regulate the formation of neutrophil extracellular traps, J. Cell Biol. 191 (2010) 677–691.
[7] S.J. Weiss, Tissue destruction by neutrophils, N. Engl. J. Med. 320 (1989) 365–376.
[8] D. Roos, C.C. Winterbourn, Immunology. Lethal weapons, Science 296 (2002) 669–671.
[9] J.M. Pullar, M.C. Vissers, C.C. Winterbourn, Living with a killer: the effects of hypochlorous acid on mammalian cells, IUBMB Life 50 (2000) 259–266.
[10] B.S. van der Veen, M.P. de Winther, P. Myeloperoxidase Heeringa, Molecular mechanisms of action and their relevance to human health and disease, Antioxidants Redox Signal. 11 (2009) 2899–2937.
[11] B. Halliwell, J.M.C. Gutteridge, The antioxidants of human extracellular fluids, Arch. Biochem. Biophys. 280 (1990) 1–8.
[12] A. Chait, T.N. Wight, Interaction of native and modified low-density lipoproteins with extracellular matrix, Curr. Opin. Lipidol. 11 (2000) 457–463.
[13] W.D. Comper (Ed.), Extracellular Matrix, Harwood Academic Press, Amsterdam, 1996.
[14] A.A. Woods, S.M. Linton, M.J. Davies, Detection of HOCl-mediated protein oxidation products in the extracellular matrix of human atherosclerotic plaques, Biochem. J. 370 (2003) 729–735.
[15] E.C. Kennett, M.D. Rees, E. Malle, A. Hammer, J.M. Whitelock, M.J. Davies, Peroxynitrite modifies the structure and function of the extracellular matrix proteoglycan perlecan by reaction with both the protein core and the heparan sulfate chains, Free Radic. Biol. Med. 49 (2010) 282–293.
[16] S. Vanichkitrungruang, C.Y. Chuang, C.L. Hawkins, A. Hammer, G. Hoefler, E. Malle, M.J. Davies, Oxidation of human plasma fibronectin by inflammatory oxidants perturbs endothelial cell function, Free Radic. Biol. Med. 136 (2019) 118–134.
[17] T. Nybo, H. Cai, C.Y. Chuang, L.F. Gamon, A. Rogowska-Wrzesinska, M.J. Davies, Chlorination and oxidation of human plasma fibronectin by myeloperoxidase-derived oxidants, and its consequences for smooth muscle cell function, Redox Biol 19 (2018) 388–400.
[18] T. Nybo, S. Dieterich, L.F. Gamon, C.Y. Chuang, A. Hammer, G. Hoefler, E. Malle, A. Rogowska-Wrzesinska, M.J. Davies, Chlorination and oxidation of the extracellular matrix protein laminin and basement membrane extracts by hypochlorous acid and myeloperoxidase, Redox Biol 20 (2019) 496–513.
[19] H. Cai, C.Y. Chuang, C.L. Hawkins, M.J. Davies, Binding of myeloperoxidase to the extracellular matrix of smooth muscle cells and subsequent matrix modification, Sci. Rep. 10 (2020) 666.
[20] H. Cai, C.Y. Chuang, S. Vanichkitrungruang, C.L. Hawkins, M.J. Davies, Hypochlorous acid-modified extracellular matrix contributes to the behavioural switching of human coronary artery smooth muscle cells Free, Radic Biol Med 134 (2019) 516–526.
[21] T.N. Wight, Arterial wall, in: W.D. Comper (Ed.), Extracellular Matrix, Harwood Academic Publishers, Amsterdam, 1996, pp. 175–202.
[22] M.C.M. Vissers, C. Thomas, Hypochlorous acid disrupts the adhesive properties of subendothelial matrix, Free Radic. Biol. Med. 23 (1997) 401–411.
[23] M.D. Rees, L. Dang, T. Thai, D.M. Owen, E. Malle, S.R. Thomas, Targeted subendothelial matrix oxidation by myeloperoxidase triggers myosin II-dependent

de-adhesion and alters signaling in endothelial cells, Free Radic. Biol. Med. 53 (2012) 2344–2356.
[24] C. Nussbaum, A. Klinke, M. Adam, S. Baldus, M. Sperandio, Myeloperoxidase: a leukocyte-derived protagonist of inflammation and cardiovascular disease, Antioxidants Redox Signal. 18 (2013) 692–713.
[25] S. Baldus, J.P. Eiserich, A. Mani, L. Castro, M. Figueroa, P. Chumley, W. Ma, A. Tousson, T.C.R. White, D.C. Bullard, M.-L. Brennan, A.J. Lusis, K.P. Moore, B. A. Freeman, Endothelial transcytosis of myeloperoxidase confers specificity to vascular ECM proteins as targets of tyrosine nitration, J. Clin. Invest. 108 (2001) 1759–1770.
[26] P. Singh, C. Carraher, J.E. Schwarzbauer, Assembly of fibronectin extracellular matrix, Annu. Rev. Cell Dev. Biol. 26 (2010) 397–419.
[27] R. Pankov, K.M. Yamada, Fibronectin at a glance, J. Cell Sci. 115 (2002) 3861–3863.
[28] W.S. To, K.S. Midwood, Plasma and cellular fibronectin: distinct and independent functions during tissue repair, Fibrogenesis Tissue Repair 4 (2011) 21.
[29] J.K. Mouw, G. Ou, V.M. Weaver, Extracellular matrix assembly: a multiscale deconstruction, Nat. Rev. Mol. Cell Biol. 15 (2014) 771–785.
[30] S.K. Akiyama, S.S. Yamada, W.T. Chen, K.M. Yamada, Analysis of fibronectin receptor function with monoclonal antibodies: roles in cell adhesion, migration, matrix assembly, and cytoskeletal organization, J. Cell Biol. 109 (1989) 863–875.
[31] O. Skaff, D.I. Pattison, M.J. Davies, Hypothiocyanous acid reactivity with low-molecular-mass and protein thiols: absolute rate constants and assessment of biological relevance, Biochem. J. 422 (2009) 111–117.
[32] J.D. Chandler, D.P. Nichols, J.A. Nick, R.J. Hondal, B.J. Day, Selective metabolism of hypothiocyanous acid by mammalian thioredoxin reductase promotes lung innate immunity and antioxidant defense, J. Biol. Chem. 288 (2013) 18421–18428.
[33] J.D. Chandler, B.J. Day, Biochemical mechanisms and therapeutic potential of pseudohalide thiocyanate in human health, Free Radic. Res. 49 (2015) 695–710.
[34] J.D. Chandler, E. Min, J. Huang, C.S. McElroy, N. Dickerhof, T. Mocatta, A. A. Fletcher, C.M. Evans, L. Liang, M. Patel, A.J. Kettle, D.P. Nichols, B.J. Day, Antiinflammatory and antimicrobial effects of thiocyanate in a cystic fibrosis mouse model, Am. J. Respir. Cell Mol. Biol. 53 (2015) 193–205.
[35] J. Talib, D.I. Pattison, J.A. Harmer, D.S. Celermajer, M.J. Davies, High plasma thiocyanate levels modulate protein damage induced by myeloperoxidase and perturb measurement of 3-chlorotyrosine, Free Radic. Biol. Med. 53 (2012) 20–29.
[36] P.E. Morgan, R.P. Laura, R.A. Maki, W.F. Reynolds, M.J. Davies, Thiocyanate supplementation decreases atherosclerotic plaque in mice expressing human myeloperoxidase, Free Radic. Res. 49 (2015) 743–749.
[37] A. Zietzer, S.T. Niepmann, B. Camara, M.A. Lenart, F. Jansen, M.U. Becher, R. Andrie, G. Nickenig, V. Tiyerili, Sodium thiocyanate treatment attenuates atherosclerotic plaque formation and improves endothelial regeneration in mice, PloS One 14 (2019), e0214476.
[38] W.M. Malisoff, D. Marine, Prevention of atherosclerosis in rabbits. I. Administration of potassium thiocyanate, Proc. Soc. Exp. Biol. Med. 35 (1936) 356–358.
[39] P.E. Nedoboy, P.E. Morgan, T.J. Mocatta, A.M. Richards, C.C. Winterbourn, M. J. Davies, High plasma thiocyanate levels are associated with enhanced myeloperoxidase-induced thiol oxidation and long-term survival in subjects following a first myocardial infarction, Free Radic. Res. 48 (2014) 1256–1266.
[40] E. Malle, L. Hazell, R. Stocker, W. Sattler, H. Esterbauer, G. Waeg, Immunologic detection and measurement of hypochlorite-modified LDL with specific monoclonal antibodies, Arterioscler. Thromb. Vasc. Biol. 15 (1995) 982–989.
[41] G. Degendorfer, C.Y. Chuang, H. Kawasaki, A. Hammer, E. Malle, F. Yamakura, M. J. Davies, Peroxynitrite-mediated oxidation of plasma fibronectin, Free Radic. Biol. Med. 97 (2016) 602–615.
[42] P.E. Morgan, D.I. Pattison, J. Talib, F.A. Summers, J.A. Harmer, D.S. Celermajer, C. L. Hawkins, M.J. Davies, High plasma thiocyanate levels in smokers are a key determinant of thiol oxidation induced by myeloperoxidase, Free Radic. Biol. Med. 51 (2011) 1815–1822.
[43] C.J. Vesey, P.V. Cole, Blood cyanide and thiocyanate concentrations produced by long-term therapy with sodium nitroprusside, Br. J. Anaesth. 57 (1985) 148–155.
[44] W.H. Tang, Y. Wu, S.J. Nicholls, S.L. Hazen, Plasma myeloperoxidase predicts incident cardiovascular risks in stable patients undergoing medical management for coronary artery disease, Clin. Chem. 57 (2011) 33–39.
[45] S.J. Nicholls, W.H. Wilson Tang, D. Brennan, M.L. Brennan, S. Mann, S.E. Nissen, S. L. Hazen, Risk prediction with serial myeloperoxidase monitoring in patients with acute chest pain, Clin. Chem. 57 (2011) 1762–1770.
[46] R.A. Koeth, V. Haselden, W.H. Tang, Myeloperoxidase in cardiovascular disease, Adv. Clin. Chem. 62 (2013) 1–32.
[47] N. Teng, G.J. Maghzal, J. Talib, I. Rashid, A.K. Lau, R. Stocker, The roles of myeloperoxidase in coronary artery disease and its potential implication in plaque rupture, Redox Rep. 22 (2017) 51–73.
[48] S. Baldus, J.P. Eiserich, M.L. Brennan, R.M. Jackson, C.B. Alexander, B.A. Freeman, Spatial mapping of pulmonary and vascular nitrotyrosine reveals the pivotal role of myeloperoxidase as a catalyst for tyrosine nitration in inflammatory diseases, Free Radic. Biol. Med. 33 (2002) 1010–1019.
[49] C. Tiruppathi, T. Naqvi, Y. Wu, S.M. Vogel, R.D. Minshall, A.B. Malik, Albumin mediates the transcytosis of myeloperoxidase by means of caveolae in endothelial cells, Proc. Natl. Acad. Sci. U. S. A. 101 (2004) 7699–7704.
[50] C. Delporte, K.Z. Boudjeltia, C. Noyon, P.G. Furtmuller, V. Nuyens, M. C. Slomianny, P. Madhoun, J.M. Desmet, P. Raynal, D. Dufour, C.N. Koyani, F. Reye, A. Rousseau, M. Vanhaeverbeek, J. Ducobu, J.C. Michalski, J. Neve, L. Vanhamme, C. Obinger, E. Malle, P. Van Antwerpen, Impact of myeloperoxidase-LDL interactions on enzyme activity and subsequent posttranslational oxidative modifications of ApoB-100, J. Lipid Res. 55 (2014) 747–757.
[51] E. Malle, G. Marsche, J. Arnhold, M.J. Davies, Modification of low-density lipoprotein by myeloperoxidase-derived oxidants and reagent hypochlorous acid, Biochim. Biophys. Acta 1761 (2006) 392–415.
[52] A.V. Sokolov, K.V. Ageeva, O.S. Cherkalina, M.O. Pulina, E.T. Zakharova, V. N. Prozorovskii, D.V. Aksenov, V.B. Vasilyev, O.M. Panasenko, Identification and properties of complexes formed by myeloperoxidase with lipoproteins and ceruloplasmin, Chem. Phys. Lipids 163 (2010) 347–355.
[53] E. Malle, G. Marsche, U. Panzenboeck, W. Sattler, Myeloperoxidase-mediated oxidation of high-density lipoproteins: fingerprints of newly recognized potential proatherogenic lipoproteins, Arch. Biochem. Biophys. 445 (2006) 245–255.
[54] L. Kubala, H. Kolarova, J. Vitecek, S. Kremserova, A. Klinke, D. Lau, A.L. Chapman, S. Baldus, J.P. Eiserich, The potentiation of myeloperoxidase activity by the glycosaminoglycan-dependent binding of myeloperoxidase to proteins of the extracellular matrix, Biochim. Biophys. Acta 1830 (2013) 4524–4536.
[55] K. Manchanda, H. Kolarova, C. Kerkenpaß, M. Mollenhauer, J. Vitecek, V. Rudolph, L. Kubala, S. Baldus, M. Adam, A. Klinke, MPO (myeloperoxidase) reduces endothelial glycocalyx thickness dependent on its cationic charge, Arterioscler. Thromb. Vasc. Biol. 38 (2018) 1859–1867.
[56] M.D. Rees, J.M. Whitelock, E. Malle, C.Y. Chuang, R.V. Iozzo, A. Nilasaroya, M. J. Davies, Myeloperoxidase-derived oxidants selectively disrupt the protein core of the heparan sulfate proteoglycan perlecan, Matrix Biol. 29 (2010) 63–73.
[57] J.W. Heinecke, W. Li, G.A. Francis, J.A. Goldstein, Tyrosyl radical generated by myeloperoxidase catalyzes the oxidative cross-linking of proteins, J. Clin. Invest. 91 (1993) 2866–2872.
[58] J.W. Heinecke, W. Li, H.L. Daehnke, J.A. Goldstein, Dityrosine, a specific marker of oxidation, is synthesized by the myeloperoxidase-hydrogen peroxide system of human neutrophils and macrophages, J. Biol. Chem. 268 (1993) 4069–4077.
[59] M.C.M. Vissers, C.C. Winterbourn, Oxidative damage to fibronectin. 1. The effects of the neutrophil myeloperoxidase system and HOCl, Arch. Biochem. Biophys. 285 (1991) 53–59.
[60] M. Kan, E.G. Shi, Fibronectin, not laminin, mediates heparin-dependent heparin-binding growth factor type i binding to substrata and stimulation of endothelial cell growth, in: Vitro Cell Dev Biol, vol. 26, 1990, pp. 1151–1156.
[61] S. Sugiyama, Y. Okada, G.K. Sukhova, R. Virmani, J.W. Heinecke, P. Libby, Macrophage myeloperoxidase regulation by granulocyte macrophage colony-stimulating factor in human atherosclerosis and implications in acute coronary syndromes, Am. J. Pathol. 158 (2001) 879–891.
[62] D.I. Pattison, M.J. Davies, Absolute rate constants for the reaction of hypochlorous acid with protein side chains and peptide bonds, Chem. Res. Toxicol. 14 (2001) 1453–1464.
[63] D.I. Pattison, M.J. Davies, Reactions of myeloperoxidase-derived oxidants with biological substrates: gaining insight into human inflammatory diseases, Curr. Med. Chem. 13 (2006) 3271–3290.
[64] D.I. Pattison, C.L. Hawkins, M.J. Davies, What are the plasma targets of the oxidant hypochlorous acid? A kinetic modeling approach, Chem. Res. Toxicol. 22 (2009) 807–817.
[65] C.C. Winterbourn, Reconciling the chemistry and biology of reactive oxygen species, Nat. Chem. Biol. 4 (2008) 278–286.
[66] H. Ostdal, H.J. Andersen, M.J. Davies, Formation of long-lived radicals on proteins by radical transfer from heme enzymes-a common process? Arch. Biochem. Biophys. 362 (1999) 105–112.
[67] O.M. Lardinois, P.R. Ortiz de Montellano, EPR spin-trapping of a myeloperoxidase protein radical, Biochem. Biophys. Res. Commun. 270 (2000) 199–202.
[68] C. Storkey, M.J. Davies, D.I. Pattison, Reevaluation of the rate constants for the reaction of hypochlorous acid (HOCl) with cysteine, methionine, and peptide derivatives using a new competition kinetic approach, Free Radic. Biol. Med. 73 (2014) 60–66.
[69] J. Yang, K.S. Carroll, D.C. Liebler, The expanding landscape of the thiol redox proteome, Mol. Cell. Proteomics 15 (2016) 1–11.
[70] M. Depuydt, J. Messens, J.F. Collet, How proteins form disulfide bonds, Antioxidants Redox Signal. 15 (2011) 49–66.
[71] P. Hagglund, M. Mariotti, M.J. Davies, Identification and characterization of protein cross-links induced by oxidative reactions, Expert Rev. Proteomics 18 (2018) 665–681.
[72] L. Carroll, D.I. Pattison, J.B. Davies, R.F. Anderson, C. Lopez-Alarcon, M.J. Davies, Formation and detection of oxidant-generated tryptophan dimers in peptides and proteins, Free Radic. Biol. Med. 113 (2017) 132–142.
[73] H. Ostdal, L.H. Skibsted, H.J. Andersen, Formation of long-lived protein radicals in the reaction between H_2O_2-activated metmyoglobin and other proteins, Free Radic. Biol. Med. 23 (1997) 754–761.
[74] C.L. Hawkins, M.J. Davies, Hypochlorite-induced damage to proteins: formation of nitrogen-centred radicals from lysine residues and their role in protein fragmentation, Biochem. J. 332 (1998) 617–625.
[75] C.L. Hawkins, M.J. Davies, Hypochlorite-induced oxidation of plasma proteins: formation of nitrogen-centred radicals and their role in protein fragmentation, Curr. Topics Biophys. 22 (Suppl. B) (1998) 89–98.
[76] L.J. Hazell, J.J. van den Berg, R. Stocker, Oxidation of low-density lipoprotein by hypochlorite causes aggregation that is mediated by modification of lysine residues rather than lipid oxidation, Biochem. J. 302 (1994) 421–428.
[77] S. Olszowski, E. Olszowska, D. Kusior, M. Piwowarczyk, T. Stelmaszynska, Hypochlorite action on plasma fibronectin promotes its extended conformation in complexes with antibodies, J. Protein Chem. 22 (2003) 449–456.
[78] C.L. Hawkins, D.I. Pattison, M.J. Davies, Hypochlorite-induced oxidation of amino acids, peptides and proteins, Amino Acids 25 (2003) 259–274.

[79] M. Karimi, B. Crossett, S.J. Cordwell, D.I. Pattison, M.J. Davies, Characterization of disulfide (cystine) oxidation by HOCl in a model peptide: evidence for oxygen addition, disulfide bond cleavage and adduct formation with thiols, Free Radic. Biol. Med. 154 (2020) 62–74.
[80] D.I. Pattison, M.J. Davies, C.L. Hawkins, Reactions and reactivity of myeloperoxidase-derived oxidants: differential biological effects of hypochlorous and hypothiocyanous acids, Free Radic. Res. 46 (2012) 975–995.
[81] S.W. Han, J. Roman, Fibronectin induces cell proliferation and inhibits apoptosis in human bronchial epithelial cells: pro-oncogenic effects mediated by PI3-kinase and NF-kappa B, Oncogene 25 (2006) 4341–4349.
[82] J. Wang, R. Milner, Fibronectin promotes brain capillary endothelial cell survival and proliferation through alpha5beta1 and alphavbeta3 integrins via map kinase signalling, J. Neurochem. 96 (2006) 148–159.
[83] D.E. Ingber, Fibronectin controls capillary endothelial cell growth by modulating cell shape, Proc. Natl. Acad. Sci. U. S. A. 87 (1990) 3579–3583.
[84] Y. Cao, X. Liu, W. Lu, Y. Chen, X. Wu, M. Li, X.A. Wang, F. Zhang, L. Jiang, Y. Zhang, Y. Hu, S. Xiang, Y. Shu, R. Bao, H. Li, W. Wu, H. Weng, Y. Yen, Y. Liu, Fibronectin promotes cell proliferation and invasion through mTOR signaling pathway activation in gallbladder cancer, Canc. Lett. 360 (2015) 141–150.
[85] M.T. Ashby, A.C. Carlson, M.J. Scott, Redox buffering of hypochlorous acid by thiocyanate in physiologic fluids, J. Am. Chem. Soc. 126 (2004) 15976–15977.